Improved Energy Harvesting Capability of Piezoelectric PVDF Films Modified by Reduced Graphene Oxide (rGO)

Liangke Wu,[a,b] Alamusi,[a] Junmin Xue,[c] Takomi Itoi,[a] Ning Hu,*[a] Yuan Li,[d] Cheng Yan,[e] Jianhui Qiu,[f] Huiming Ning,[a] Yaolu Liu,[a] Yiqi Wang,[g] Xu Han,[g] Weifeng Yuan,[h] Christinana Chang,[i] Satoshi Atobe[j] and Hisao Fukunaga[j4]

Piezoelectric energy harvesters can be used to convert ambient mechanical energy into electrical energy and power small autonomous devices. In recent years, massive effort has been made to improve the energy harvesting ability in piezoelectric materials. In this study, graphene was added into PVDF (polyvinylidene fluoride) to improve the piezoelectricity of PVDF. Open-circuit voltage and energy harvesting experiments showed a remarkable enhancement in the piezoelectric properties of PVDF/graphene composite at an optimal loading of graphene (i.e., 0.05 wt.%). Compared to pristine PVDF, the open circuit voltage, AC (alternating current) harvested energy and DC (direct current) harvested energy in the PVDF/graphene composite was increased by 105%, 153%, and 233%, respectively, indicating a great potential for a broad range of applications.

1 Introduction

With the development of electronics technology, the power consumption of portable devices decreases continuously, thus the self-power function becomes feasible. Moreover, in some special situations, replacement of batteries is not convenient or costly expensive.[1] Therefore, energy harvesters converting ambient energy, e.g., vibration, into electrical energy, have been developed. Compared to battery-powered devices, these devices are more environment-friendly and have longer operating lives, attracting increased attention to researchers.[2,3] Among various energy harvesting systems, piezoelectric material based devices have many advantages.

To date, PZT (Lead Zirconate Titanate) is the most commonly used piezoelectric material in the energy harvesters[4-8] In spite of its good performance, PZT is fragile and susceptible to fatigue. [9] In addition, the toxicity of lead oxide in PZT raised significant health and environment concerns. Therefore, a great technical challenge in development of energy harvesting technologies is to replace PZT with environment friendly materials such as new lead-free piezoelectric materials. Possible candidates included piezoelectric polymers (e.g. PVDF and PVDF copolymer) as they are not toxic, recyclable, resistant to halogen, acid and fatigue.[10] Moreover, they are highly flexible, and can be applied on the curved structural surfaces[10].For instance, Elvin *et al.* fabricated wireless strain sensor using PVDF films[11]. Through a simple bending experiment, the characteristics of the self-power strain sensor related to frequency and applied load were investigated. Wireless communication was also realized. In addition, it can be also used to power a rechargeable battery. A bioinspired piezo-leaf architecture converting wind energy into electrical energy was studied by Li *et al.*[12] In their experiment, the maximum output power and maximum power density approached 600 μW and 2.0 mW/cm^3, respectively. Granstrom *et al.*[13] developed a novel strap and the maximum harvested power reached 3.75 mW and the maximum power density approached 2.7 mW/cm^3. Since the mechanical properties of PVDF type polymer are very similar to those of nylon, i.e., the material with backpack strap, it is then possible to replace nylon with PVDF for enhanced energy harvesting capacity. Liu *et al.*[14] investigated on the active energy harvesting circuit using switch-mode power electronics to control the voltage and/or charge on a piezoelectric device to increase energy conversion efficiency and demonstrated it with a multilayer PVDF polymer device. The experiments showed that the active energy harvesting approach generated about 5 times of energy for the same mechanical displacement compared to the passive rectifier-based circuit.

As described above, most reports focus on prototyping PVDF films, utilizing more effective energy harvesting circuits, or modeling the piezoelectric devices. However, a little has been done to improve the energy harvesting capability in PVDF's. In this study, reduced graphene oxide (rGO) is added into PVDF to fabricate PVDF composite films. The experiment showed that the energy harvesting or conversion capability is dramatically improved by adding graphene as compared to pristine PVDF films. X-ray diffraction (XRD) and Fourier transform infrared spectroscopy (FTIR) were used to uncover the mechanism of the increase of PVDF composite's piezoelectricity and energy harvesting capability. The variation of internal crystal structure induced by graphene, especially the piezoelectric crystal content, i.e., β phase content in PVDF is considered to be the possible reason. Moreover, a theoretical model for predicting the harvested power was also used to explain the observed experimental phenomena. We believe that this new and powerful piezoelectric polymer composite provides an effective means to fabricate better energy harvested devices in the future.

2 Experiments

2.1 Materials

Reduced graphene oxide (rGO) was prepared by a modified Hummers method[20] from natural flake graphite powder. The process included two steps: 1) Oxidation and exfoliation, 1 g and 1 g $NaNO_3$ were mixed and then put into 46 mL concentrated H_2SO_4 (98%), an ice bath was adopted to keep the temperature below °C for h . The mixture was magnetically stirred for 1 hour following gradual addition of 6 g $KMnO_4$ under stirring. Afterwards, the mixture was kept in a water bath of 35 °C for 24

h. Successively, 40 mL H_2O was added while the temperature of the mixture rose to about 80 °C. 100 mL H_2O and 20 mL 20% H_2O_2 solution were added into the mixture in succession to dilute it. After stirring of 30 min, the mixed solution was centrifuged to gather the intermediate product, i.e. graphene oxide. The graphene oxide was washed with 4% HCl solution and deionized water for several times. Afterwards, the graphene oxide was kept in an oven at 70 °C for 4 days for drying. 2) Reduction, prepared GO was dispersed in ethylene glycol by ultrasonication. The mixture was put into a 125 mL Teflon-lined stainless steel autoclave in an air-flow electrical oven at 200 °C for 4 days for reduction, then the desired reduced graphene oxide was gathered by centrifugation and rinsed with pure ethanol for 3 times.

Fig. 1 is an AFM (atomic force microscopy, Veeco NanoScope IV Multi-Mode with the tapping Mode) image of GO sheets of size as about 5 μm. From the image, we see that the average thickness of the rGO sheet is 1.052 nm. Compared to the theoretical value 0.78 nm, it is slightly larger, which may result from the oxygen-containing groups on the graphene surfaces.

The graphene flakes were then observed using a scanning electron microscopy (SEM, Hitachi SU-70) as shown in figure 2 with different magnifications, in which very thin graphene sheets can be identified. Furthermore, the graphene flakes were characterized by a transmission electron microscopy (TEM, JEOL 100CX instrument) as shown in figure 3(a). Some graphene flakes are composed of 1-10 individual sheets and others may have more sheets, approximately up to 50.

To observe the atomic structure of suspended rGO in details, TEM images (JEM-2100F) are shown in figure 3(b) with an insert of FFT (Fast Fourier Transform) processed image. We can see that the graphene only contains some small ripples and has a very high crystallinity (hexagonal lattice structure).

As for PVDF, the PVDF-HFP (Poly (vinylidene fluoride-co-hexafluoropropylene)) was supplied by Arkema Inc., and the Dimethylformamide (DMF) was obtained from Wako Pure Chemical Industries, Ltd. The properties of PVDF-HFP are listed below in Table 1. It was used as received.

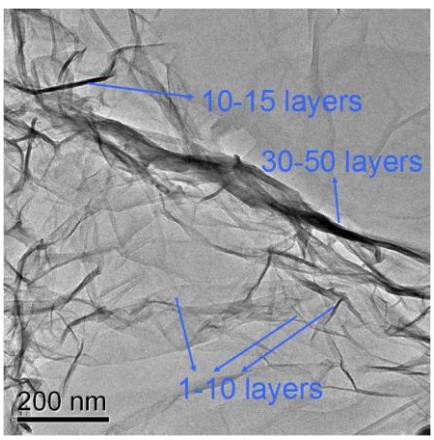

(a)

Table 1 Properties of PVDF-HFP

Density	1.76 ~1.8 g/cm^3
Refraction index	1.41
Melt viscosity	2300~2700 Pa • s (232℃,100 s-1)
Melting temperature	140~145 ℃
Water absorption	0.03%
Melt flow rate	3.5~7.5 g/10min (232 ℃)

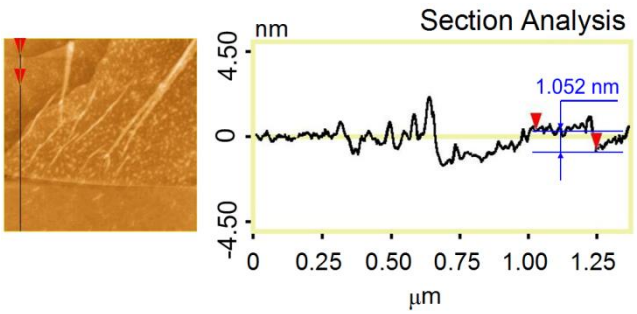

Fig. 1 AFM image of graphene

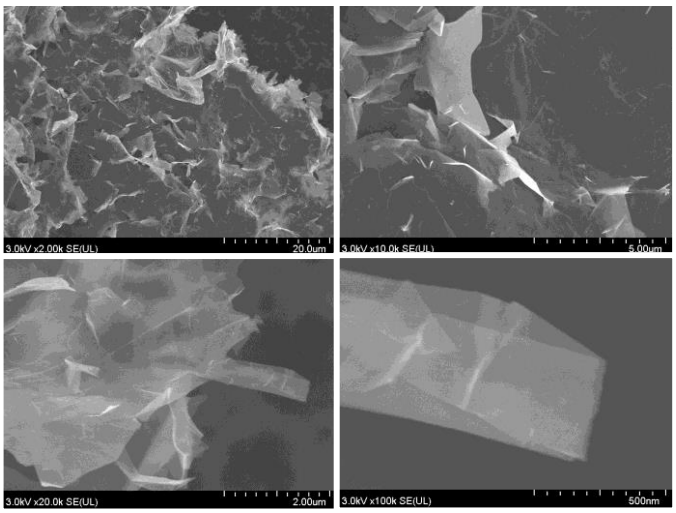

Fig. 2 SEM images of graphene

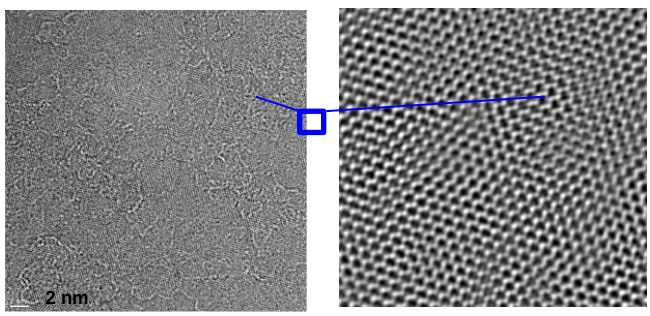

(b)

Fig. 3 (a) TEM image of graphene; (b) TEM image of graphene with an insert of FFT image

2.2 Preparation of PVDF/Graphene Films

The whole fabrication process of the piezoelectric composite films is shown in Fig. 4. The solution cast method was used to

prepare PVDF/graphene films. The graphene was added into DMF (m = 30 g) and mixed by sonication (UH-600, SMT Co. Ltd.) for 15 minutes. After that, 10g PVDF was dissolved in the solution and mixed by sonication for 5 min and then by the rotation-revolution mixer for 10 min at a revolution speed of 2000 rpm. The as-produced solution was then poured onto an Al plate for curing at 90 °C for two hours. The sample was then cut into smaller films of size 3 cm × 3 cm.

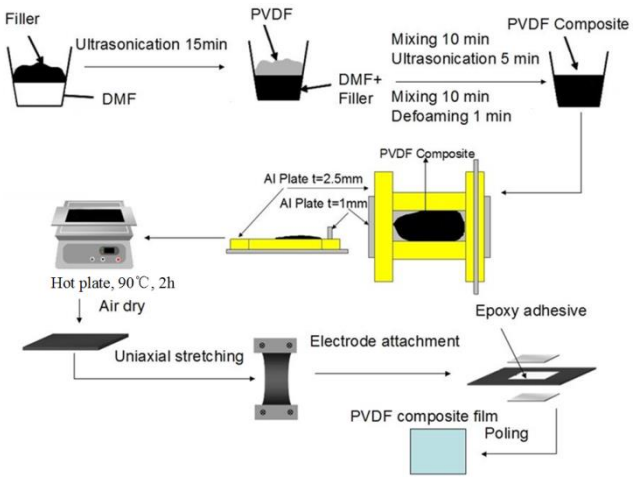

Fig. 4 Preparation of PVDF composite films

The film was stretched to induce PVDF phase transformation. It was reported that a stretching ratio of 4 is sufficient for the phase transformation[15]. In this study the stretching ratio was selected to be 5. After stretching, two electrodes were attached to both sides of the film.

The poling was carried out in silicon oil at room temperature. The step-wise poling method[16] was employed and the applied electrical field ranged from 20 MV/m to 60 MV/m. The relationship between time and applied electrical field is shown in Fig. 5.

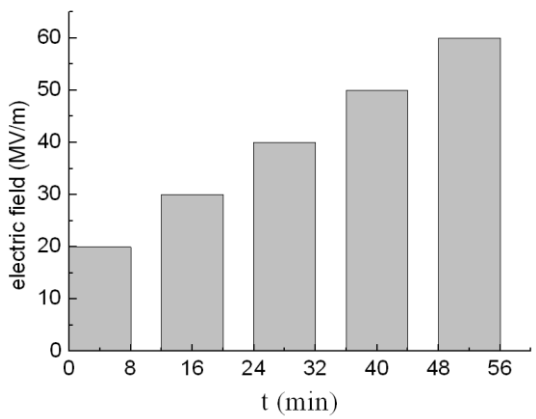

Fig. 5 Relationship between time and applied electrical field

The PVDF composite films with weight content 0, 0.05%, 0.1% and 0.2% graphene are notated as PVDF(0), PVDF(0.05), PVDF (0.1), PVDF(0.2), respectively. The average thickness of the films is listed in Table 2.

Table 2 The average thickness of films

Content (wt.%)	0	0.05	0.1	0.2
Thickness(μm)	82.3	76.7	81.5	78.6

2.3 Open circuit voltage measurements

2.3.1 Experiments

To evaluate the piezoelectricity of the PVDF composite, the open circuit voltage of the PVDF composite films was measured. The measurement setup is illustrated in Fig. 6.

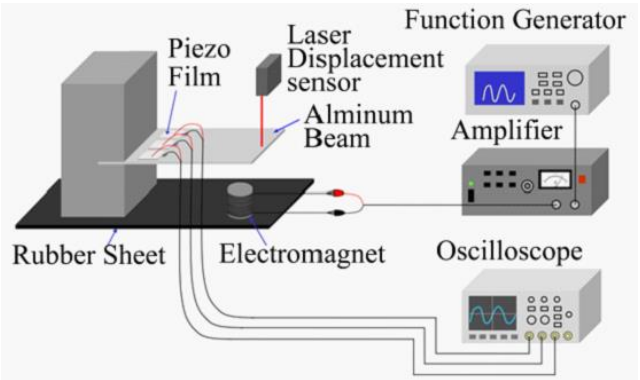

Fig. 6 Experiment setup of open circuit voltage measurement

Three pieces of PVDF composite films were attached on the Al plate (10 cm × 20 cm × 1 mm) by epoxy resin. The electromagnet was excited by an amplified sinusoidal signal produced by the function generator and interacted with a permanent magnet attached on the underside of the Al plate (not shown). As a result, the Al plate vibrated at the same frequency of the sinusoidal signal. To induce the maximum displacement at the free end, the frequency of the sinusoidal signal was set to be the same as the natural frequency of the Al plate, i.e. about 25 Hz. With the vibration of the Al plate, the length of the films varied periodically. Because of the piezoelectricity of the films, voltage was generated on the two sides of the films and was measured by oscilloscope. The displacement of the free end of the Al plate was measured by the laser sensor. For effective comparison of different films, the displacement of the plate in all tests was set to 1 mm.

2.3.2 Results and Discussion

The 31 charge generation mode ("3" and "1" indicates the directions, see Fig. 7.) of a piezoelectric element due to the relationship between stress and charge is shown in Fig. 7.

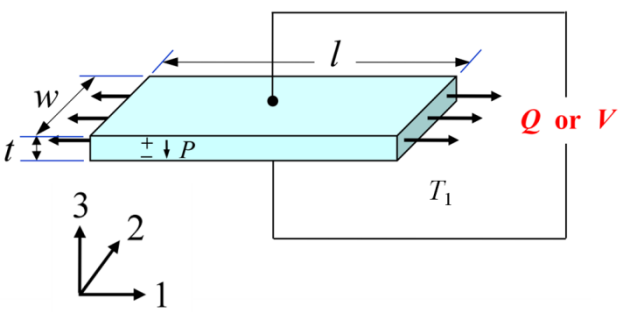

Fig. 7 Relation between stress and charge

The relation between stress T_1, strain S_1, electric field E_3 and electric flux density D_3 is expressed by

$$\begin{cases} S_1 = s_{11}^E T_1 + d_{31} E_3 \\ D_3 = d_{31} T_1 + \varepsilon_{33}^T E_3 \end{cases} \quad (1)$$

In Eq. (1), s_{11}^E is the compliance of the short circuit piezoelectric element, d_{31} is the piezoelectric strain constant, and ε_{33}^T is the permittivity when the stress is 0. Since the electric field along the 3 direction,E_3, is 0, Eq. (1) can be rewritten as

$$D_3 = d_{31} T_1 = \frac{Q}{A_{ele}} \quad (2)$$

in which A_{ele} is the area of the electrode. According to Eq. (2), the charge across the two sides of the films can be calculated by

$$Q = A_{ele} T_1 d_{31} \quad (3)$$

The following notations will be taken: C_0 for the capacitance of the film, E' for the Young's modulus, ε' for the corresponding strain in the 1 direction, g_{31} for the piezoelectric voltage constant and Δl for the displacement along the 1 direction, t for the thickness of the piezoelectric film. The open circuit voltage produced is given as

$$V = \frac{Q}{C_0} = \frac{T_1 d_{31} t}{\varepsilon_{33}^T} = E' \varepsilon' g_{31} t = \frac{E' g_{31} \Delta l t}{l} \quad (4)$$

From Eq. (4), it can be argued that the voltage is proportional to the thickness t or the displacement of the tip of the Al plate Δl.

For periodical voltage, the effective voltage is defined as

$$V_{rms} = \sqrt{\int_0^T \frac{V^2 dt}{T}} \quad (5)$$

in which T is the period. Since the instantaneous voltage is proportional to the thickness and displacement (Eq.4), it can be easily concluded that the effective voltage is also proportional to thickness and displacement from Eq. (5). As the output voltage in the experiment is sinusoidal, V_{rms} equals $0.707 V_{max}$.

As the thicknesses of films vary from each other and the displacements of the free end of the Al plates are also slightly different from each other, for comparison of the open circuit voltage the nominal film thickness and plate tip displacement were selected to be $t_0 = 100\ \mu m$ and $u_0 = 1\ mm$, respectively. For each sample, the open circuit voltage was used to calculate the calibrated open circuit voltage, V_c, by the following equation

$$V_c = \frac{V_{rms}}{\left(\frac{tu}{t_0 u_0}\right)} \quad (6)$$

The results of the open circuit voltage measurements are shown in Fig. 8.

From Fig. 8, it can be seen that an addition of a small amount of graphene can improve the piezoelectricity significantly. When the content of the graphene is 0.05 wt.%, the open circuit voltage increases to 205% of the pure PVDF films; however, when the content is 0.2 wt.%, the increase ratio is just 26%, indicating that too much filler will hinder the transformation of PVDF crystal structures from the α from to the β form, which depends the piezoelectricity of the films. From Eq. (4), for the films of 0.05 wt.% filler, as E' remains nearly the same, the enhancements in piezoelectricity are mainly due to the increase of the piezoelectric voltage constant, g_{31}. However, for the films of 0.2 wt.% filler, E' changes significantly and may be the reason for the increase in open circuit voltage.

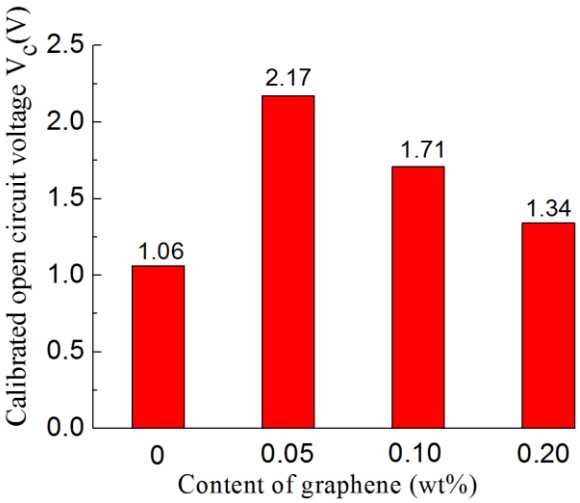

Fig. 8 The calibrated open circuit voltage of films

2.4 Harvested energy of AC circuit

2.4.1 Experiments

The standard energy harvesting alternating current (AC) circuit shown in Fig. 9 was used to measure the harvested energy from the PVDF films in a closed circuit, rather than the open circuit scheme described previously in this paper.

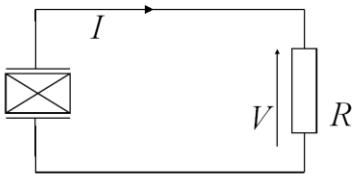

Fig. 9 Standard AC circuit

Three films were attached on the plate in parallel to increase the electro-mechanical coupling factor. The plate was excited at the primary natural frequency at a nominal displacement of 1.5 mm. Under the above conditions, the voltage, V, across the circuit load, R, was measured and used to calculate the harvested power.

2.4.2 Results

The harvested power can be calculated as

$$P = \frac{V_{rms}^2}{R} \quad (7)$$

in which V_{rms} is the root mean square voltage (also called the effective voltage) and R is the resistance.

The density of harvested power is calculated by

$$D_e = \frac{P}{V_{ol}} \quad (8)$$

in which V_{ol} is the total volume of the three films.

The density of harvested power of the AC circuit is shown in Fig. 10.

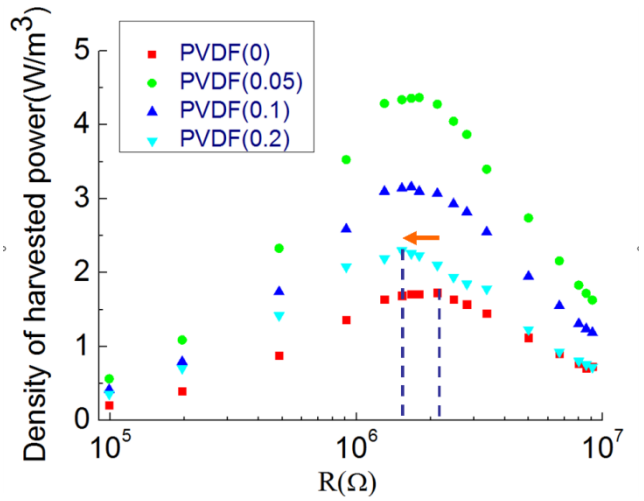

Fig. 10 Results of density of harvested power measurements

From Fig. 10, it can be seen that the density of the harvested power of the PVDF (0.05) films is the highest and is about 253% of that of the neat PVDF(0) films. Additionally, the resistance at the optimal harvested energy density decreases with increasing graphene content.

2.4.3 Discussion

The theoretical model proposed by Guyomar[17] was used to analyze the increase of the density of harvested power.

The output power of a piezoelectric element can be described as

$$P = \frac{R\alpha^2}{1+(RC_0\omega)^2}\frac{F_m^2}{2C} \tag{9}$$

where R is the resistance, C_0 is the clamped capacitance of piezoelectric elements, ω is the angular frequency, F_m is the external force amplitude, C is the damping due to the mechanical losses of the structure, α is the force factor, e_{31} is the piezoelectric constant. Thus, the optimal resistance and the maximum power is

$$R_{opt} = \frac{1}{C_0\omega}, P_{max} = \frac{\alpha^2}{4C_0\omega}\frac{F_m^2}{C^2} \tag{10}$$

Then, the maximum density of harvested power is

$$D_{emax} = \frac{\alpha^2}{4C_0\omega}\frac{F_m^2}{V_{ol}C^2} \tag{11}$$

Also, α and c_0 can be given as

$$\alpha = e_{31}w, C_0 = \varepsilon_{33}^S\frac{wl}{t} \tag{12}$$

Using Eq. (12), Eq. (11) can be rewritten as

$$D_{emax} = \frac{e_{31}^2w^2}{4C_0\omega}\frac{F_m^2}{V_{ol}C^2} \tag{13}$$

where w, l and t are the width, length and thickness of the piezoelectric element, respectively. ε_{33}^S is the clamped permittivity of the piezoelectric element.

If the plate is vibrated near the primary frequency, the following equation can be used to describe the relation between α and C_0.

$$\alpha = \gamma C_0 \tag{14}$$

where γ is the ratio of open circuit voltage to the displacement of the free end of the Al plate.

From Fig. 10, it can be seen that the resistance at optimal density of harvested energy decreases with the increase of graphene content. From Eq. (10), since the frequency of the plate nearly remains the same (26 Hz), the clamped capacitance C_0 of the piezoelectric elements must increase for all composite films. For the films of 0.05 wt.% filler, since the maximum power increases according to Eq. (10), the force factor α must increase. From Eq. (12), it is believed that the piezoelectric constant e_{31} increases, resulting in increased open circuit voltage and harvested energy.

2.5 Harvested energy of DC circuit

2.5.1 Experiments

The setup for the DC circuit harvested energy measurements is similar to that of the AC circuit measurements, but uses the DC circuit presented in Fig. 11 instead of the AC circuit.

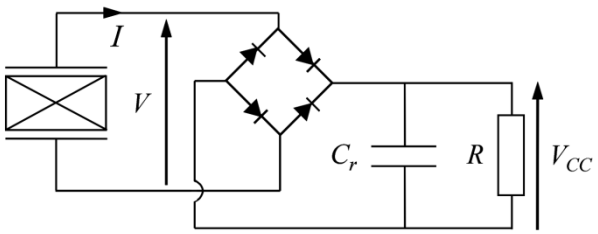

Fig. 11 Standard DC energy harvesting circuit

The rectifier diode group is DX5342 and the capacitance C_r is 33 μF. Three pieces of film were attached on the plate and the plate was excited at the primary frequency in parallel to increase the electro-mechanical coupling factor. The displacement of the tip was 1.5 mm.

2.5.2 Results

The harvested power is calculated by

$$P = \frac{V_{cc}}{R^2} \tag{15}$$

where V_{cc} is the direct voltage and R is the resistance. The density of harvested energy is defined as

$$D_e = \frac{P}{V_{ol}} \tag{16}$$

where V_{ol} is the total volume of the three films.

The Fig. 12 shows the density of harvested power collected for the DC tests.

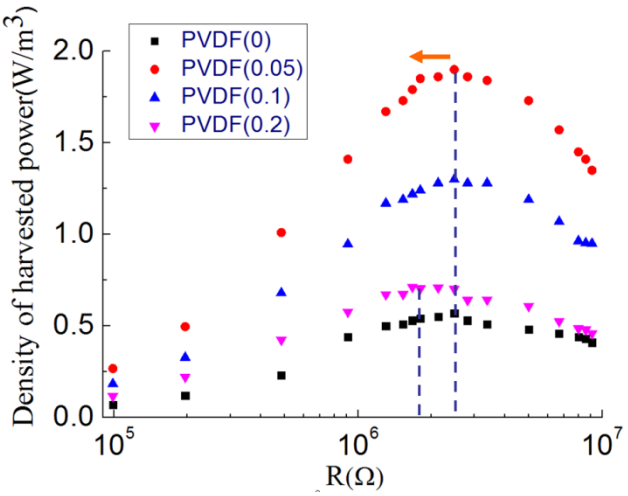

Fig. 12 Results of density of harvested energy measurements

From Fig. 12, the results show that the density of harvested energy of films of 0.05 wt.% graphene is about 333% of that of PVDF(0) films. Furthermore, the optimal resistance of PVDF(0.2) is less than that of films of other contents, but the peak is not so obvious. Since there is a saturation power value for the DC circuit, the harvested energy remains near the saturation power value at a wide range of resistances; thus, the optimal resistance is not so obvious.

2.5.3 Discussion

According to the model proposed by Guyomar *et al.*[17], the optimal resistance and the maximum power are

$$R_{opt} = \frac{\pi}{2C_0\omega}, P_{max} = \frac{\alpha^2}{2\pi C_0\omega}\frac{F_m^2}{C^2} \quad (17)$$

Comparing Eq. (10) and Eq. (17), it is concluded that the optimal resistance R_{opt} of the DC circuit is larger than that of the AC circuit by π/2 and that the maximum power is much less than that of AC circuits. The experimental results in Figs. 10 and 12 show the same trend, but do not match quantitatively with the model of Guyomar *et al.*[17] from the aspect of R_{opt}. The threshold voltage of the rectifier diode group is about 0.3-0.4 V, which is comparable to the open circuit voltage. Thus, in the model proposed by Guyomar, the assumption that the rectifier group is an ideal one with threshold voltage of 0 V is unreasonable, resulting in its disagreement with the experimental results.

3 Crystallinity Analysis

As mentioned, the piezoelectricity of PVDF depends on the content of the piezoelectric β phase. The results of open circuit voltage and harvested power indicated that there must be different phase transformation processes from α form to β form to account for the experimental data variations among films of different graphene contents. In this study, XRD and FTIR were used to investigate the crystallinity in composites to confirm the effects of the graphene fillers on the crystal transformation.

3.1 XRD

The XRD was carried out by MPX-3A (X-ray Diffractometer , Mac Science Ltd.) with CuKα at 40 kV and 30 mA. The angle 2θ ranged from 15° to 30°, the step was 0.02°, and the scanning speed was 1°/min.

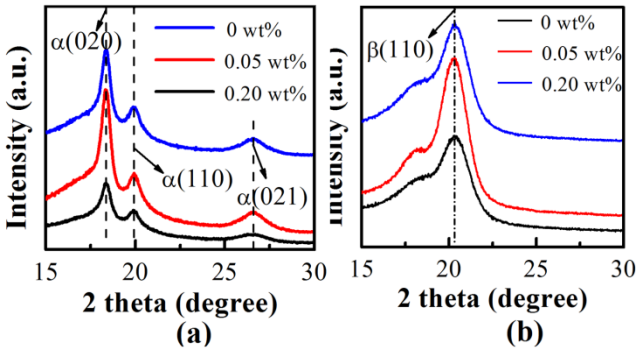

Fig. 13 X-ray diffraction spectra of PVDF/graphene films: (a) before stretching; (b) after stretching

Fig. 13 is the XRD results of the PVDF composite films before and after stretching. In this figure, the peaks at 18.4°, 20.0°, 26.5°, which correspond to (100), (110), (021) of the α form crystallinity[18], are observed. Meanwhile, a peak of 20.6°[18], which corresponds to the (110) of β crystallinity, does not exist. The result indicates that before stretching, the α form dominates the film. However, the XRD spectrum of stretched films is quite different. The peaks related to the α form nearly disappear, indicating that there is a complete phase transformation during the stretching.

3.2 FTIR

FTIR was used for further investigation of crystallinity. In the FTIR spectra analysis, the thickness of the sample was 10 μm. The spectrum ranges from 1000 to 600 cm^{-1} with a resolution of 4 cm^{-1} and an aperture of 25×100 μm. The FTIR spectrum of PVDF/graphene films is shown in Fig. 14. In Fig. 14(a), the peaks of 615, 765, 975 cm^{-1}, which correspond to the α form crystallinity[19] and the peak of 840 cm^{-1}, which corresponds to the β form crystallinity[19], both exist. In the stretched films, the peaks correspond to β form crystallinity increases significantly; in contrast, the peaks correspond to α form crystallinity decrease – some peaks even disappear. This transition indicates that after stretching, a majority of α form has been converted to β form. The result is consistent with that of the XRD analysis.

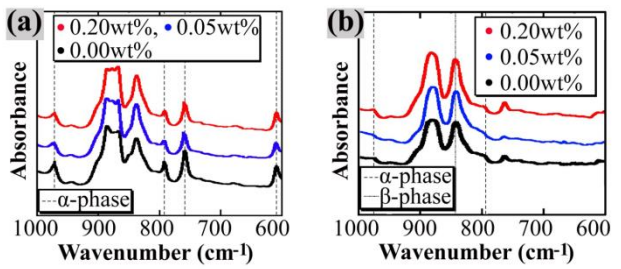

Fig. 14 FTIR spectra of PVDF/graphene nanocomposites: (a)before stretching; (b) after stretching

3.3 Discussion

From XRD and FTIR spectra results, it is concluded that prior to

stretching the films, both α and β form crystallinities existed, but α form dominated in the films. However, after stretching the films, the α form crystals were converted to β form. As a result, the piezoelectricity was improved due to stretching.

As for the role played by graphene in PVDF phase transformation, it can be clarified from the following three aspects:

1) Due to addition of graphene, which works as a crystal nucleation, more α form crystal may be formed easily before stretching, leading to more β form crystal after stretching if the transformation rate remains the same.
2) The phase transformation mainly depends on the stress distribution. In the pure PVDF films, the transformation rate depends on the stress applied on the molecular chains and the stretching ratio. When the graphene is added to the polymer, the high stress concentration on the interface between graphene and polymer chain is induced. It can enhance the phase transformation efficiency.
3) However, too many nucleation nanofillers hinder the elongation of the macromolecular chain during phase transformation. Thus, the films of content at 0.1 wt.% and 0.2 wt.% graphene displayed degraded piezoelectric performance compared to films of lower graphene content. Another possible reason is the charge accumulation at nanofiller/β crystallinity/α crystallinity interfaces results in a depolarization field exceeding the coercive field in composite films.[21]

4 Conclusions

PVDF composite films with various contents of graphene were prepared and their piezoelectricities were measured by open circuit voltage test and harvested energy measurements. The results showed that a small addition of graphene can significantly increase the open circuit voltage and harvested power, due to the improved piezoelectricity of PVDF. Especially at a graphene content of 0.05 wt.%, the films performed best. The XRD and FTIR spectra analysis confirmed the nucleation action of graphene in the formation of β phase crystal in PVDF. It is also worthy to note that a too high content of graphene will hinder the nucleation development because the free area for β phase development will be much smaller.

Notes and references

[*a]*Department of Mechanical Engineering, Chiba University, 1-33 Yayoi-cho, Inage-ku, Chiba City, Chiba 263-8522, Japan. Tel (Fax): 81-43-290-3204.*
E-mail: huning@faculty.chiba-u.jp
Email: alamusi@chiba-u.jp
Email: ninghuiming@gmail.com
Email: liuyaolu@graduate.chiba-u.jp
[b]*Department of Mechanical Engineering, Zhejiang University, 38 Zheda Road, Hangzhou, Zhejiang, 310027, P.R. China.*
E-mail: wuliangke@gmail.com
[c]*Department of Materials Science, National University of Singapore, 21 Lower Kent Ridge Road, Singapore 119077.*
E-mail: msexuejm@nus.edu.sg
[d]*Department of Nanomechanics, Tohoku University, 6-6-01 Aramaki-Aza-Aoba, Aoba-ku, Sendai 980-8579, Japan.*
E-mail: liyuan@ism.tohoku.ac.jp
[e]*School of Chemistry, Physics and Mechanical Engineering, Science and Engineering Faculty, Queensland University of Technology, 2 George Street, GPO BOX 2434, Brisbane, Australia*
[f]*Department of Machine Intelligence and Systems Engineering, Akita Prefectural University, Akita 015-0055, Japan.*
E-mail: qiu@akita-u.ac.jp
[g]*College of Mechanical and Vehicle Engineering, Hunan University, Changsha, Hunan 410082, China.*
Email: magicgog@hotmail.com
Email: hanxu@hnu.edu.cn
[h]*School of Manufacturing Science and Engineering, Southwest University of Science and Technology, 59 Qinglong Road, Mianyang 621010, P.R.China.*
Email: yuanweifeng@swust.edu.cn
[i]*Department of Mechanical Engineering, University of Houston, Houston, TX, USA.*
E-mail:cchang2@uh.edu
[j]*Department of Aerospace Engineering, Tohoku University, 6-6-01 Aramaki-Aza-Aoba, Aoba-ku, Sendai 980-8579, Japan.*
E-mail:atobe@ssl.mech.tohoku.ac.jp
E-mail:fukunaga@ssl.mech.tohoku.ac.jp

1 E. D. Ramirez, Energy Harvesting from Body Motion Using Rotational Micro-generation, Dissertation of Michigan Technological University, 2010.
2 A. Erturk, Electromechanical Modeling of Piezoelectric Energy Harvesters, Dissertation of Virginia Polytechnic Institute and State University, 2009.
3 Shashank, Appl. Phys. Lett. , 2005, **87**, 184101
4 X. Chen, S. Xu, N. Yao and Y. Shi, Nano Letters, 2010, **10**, 2133-2137
5 J. P. Lynch, A. Sundararajan, H. Sohn, G. Park, C. Farrar and K. H. Law, Proceedings of the International Workshop on Smart Materials and Structures Technology,
6 P. D. Mitcheson, G. K. Rao, T. C. Green, Proceedings of the IEEE, 2008, **96**, 1457-1486
7 Y. K. Ramadass, A. P. Chandrakasan, IEEE Journal of Solid State Circuits, 2010, **45**, 189-204
8 S. P. Beeby, M. J. Tudor, N. M. White, Meas. Sci. Technol., 2006, **17**, R175-R195
9 D. Guo, L. Li, Z. Gui, C. Nan, Materials Science and Engineering, 2003, **B99**, 25-28
10 F. Liu, N. A. Hashim, Y. Liu, M. R., M. Abed and K. Li, Journal of Membrane Science, 2011, **375**, 1-27
11 N. G. Elvin, A. A. Elvin and M. Spector, Smart Mater. Struct., 2001, **10**, 293-299
12 S. Li, J. Yuan and H. Lipson, Journal of Applied Physics, 2011, **109**, 026104
13 J. Granstrom, J. Feenstra, H. A. Sodano and K. Farinholt, Smart Mater. Struct., 2007, **16**, 1810-1820
14 Y. Liu, G. Tian, Y. Wang, J. Lin, Q. Zhang and H. F. Hofmann, Journal of Intelligent Material Systems and Structures, 2009, **20**, 575-585
15 V. Sencadas, R. G. Jr. and S. Lanceros-Mendez, Journal of Macromolecular Science,Part B: Physics, 2009, **48**, 514-525
16 K. L. Ng, H. L. W. Chan and C. L. Choy, IEEE Transactions on Ultrasonics, Ferroelectrics and Frequency Control, 2002, **47**, 1308-1315
17 D. Guyomar, A. Badel, E. Lefeuvre and C. Richard, IEEE Transactions on Ultrasonics, Frequency Control, 2005, **52**, 584-595
18 S. Yu, W. Zheng. W. Yu, Y. Zhang, Q. Jiang and Z. Zhao, Macromolecules, 2009, **42**, 8870-8874
19 A. Salimi and A. A. Yousefi, Polym. Test, 2003, **22**, 699-704
20 W. S. HUMMERS and R. E. Offeman, J. Am. Chem. Soc., 1958, **80**, 1339-1339
21 G. H. Kim, S. M. Hong and Y. Seo, Phy. Chem. Chem. Phys. 2009, 11,11506-11512